Available online at www.elixirpublishers.com (Elixir International Journal)

Applied Chemistry

Elixir Appl. Chem. 64 (2013) 19054-19059

ISSN: 2229-712X

Synthesis of linear unbranched polymers chain free of macrocyclic species and oligomers based on chloro-monomers and TTSBI

Fadi Ibrahim

Department of Chemistry, Abdul Latif Thanian Al-Ghanim School Kuwait, Ardeia, part 6, Fst str, Kuwait.

ARTICLE INFO

Article history:

Received: 3 September 2013;

Received in revised form:

25 October 2013;

Accepted: 31 October 2013;

Keywords

Linear polymers,
Chlorinated monomers,
Membrane,
Molecular weight distribution,
Hydrogen adsorption.

ABSTRACT

A high molecular weight linear unbranched polymers free of macrocycles has been synthesized by long polycondensation time under high-intensity mixing conditions at about 80°C between cheaper chloro-monomers (instead of fluorinated monomers)[1] and 5,5',6,6'-tetrahydroxy-3,3,3',3'-tetramethylspirobisindane (TTSBI). From the porosity analysis, it is clear that the prepared polymers are analogous to polymers of intrinsic microporosity (PIMs) with high surface area (500-700 m^2/g). The hydrogen storage capacity of the prepared PIM-Cl(1-7) and were promising (up to 1.19 wt%, 77 K, at 1.13 bar). The results of this study demonstrate that controlling polymerization condition can provide a uniform microporous morphology in the target polymers.

Introduction

The preparation of purely microporous polymers without the assistance of molecular template is becoming a fast developing area in nonmaterial's research and many approaches have been used to develop various insoluble network organic microporous polymers such as hyper cross-linked polymers (HCP)[1,2], triptycene-based PIM (Trip-PIM)[3], conjugated microporous polymers (CMP)[4], organic framework polymer (OFP)[5], porous organic polymers (POP)[6] and microporous polyimide networks[7,8] with high specific surface. The most outstanding representation for this kind of materials are the polymers of intrinsic microporosity (PIMs)[9] developed by McKeown and Budd et al with high surface areas in the range of 500-900 m^2/g.[10, 11] The ideal structure of this ladder polymer result from polycondensation reactions of bisphenols and bi-halo aromatics is a linear unbranched chain free of macrocyclic species and crosslinking. The formation of this ladder polymer not pass forward and a lot of cyclic, oligomers, and branched by-product may formed as schematically presented in Scheme 1.

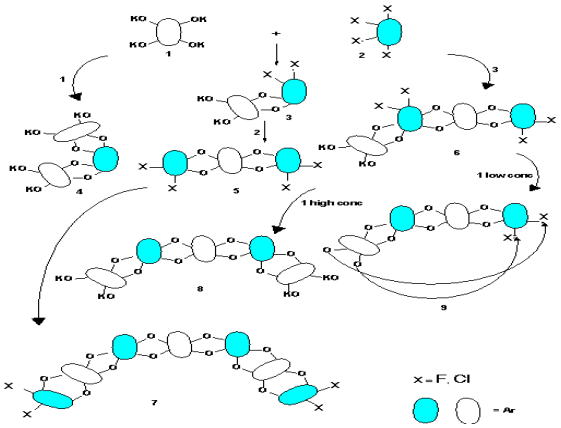

Scheme 1. Schematically presented of ladder polymer with a simple model help to explain how the cyclic species are formed in the reaction system

Although the reaction is complicated due to the monomers multiple reactive groups, the simple model can help to explain how the cyclic species are formed in the reaction system.[12-16] As the reaction is irreversible, no equilibrium exists in this polymerization process. The first step reaction product is the intermediate **3**, which is much more reactive, due to its higher solubility, than the monomer salt **1**. Therefore, the intermediate **3** preferentially reacts with the very reactive tetrachloro aromatic **2** to give **5** or with itself to yield **6**. Under normal stirring conditions where **1** very slowly goes into solution, its concentration is low so that the intermediate **6** could react with **5** to give **7** and with itself to yield a cyclic **9**. Higher analogs of **6** could also give cyclic products when the concentration of **1** in solution is low, thus contributing to a broad molecular weight distribution. Under high-intensity mixing conditions, the concentration of **1** is high so that it is not only able to react with **6** and its higher analogs to give the soluble intermediate **8**, but also with intermediates **3**, **5** and **7** to form linear oligomers, and subsequently high molecular weight polymers. It has been observed in classic polycondensation reactions of bisphenols and bichloro aromatics (as shown in Scheme 2) for the production of poly(aryl ethers) that a large amount of macrocyclic oligomers were formed.

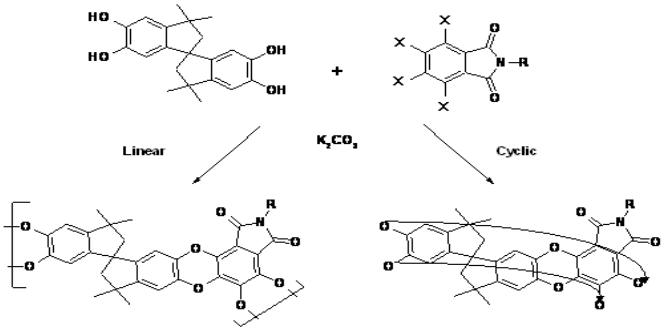

Scheme 2. Formation of both linear and cyclic compound (related to dilution conditions) in the reaction mixture

Tele:

E-mail addresses: fed_ooo@yahoo.com

During the intial stages of the reaction, the bisphenol reacted with sodium or potassium carbonate (or hydroxide) to give a number of salt precipitates which hindered stirring of the reaction mixture. To avoid formation of cyclic compounds in the reaction mixture (as shown in Scheme 2), a high dilution (created by poor solubility of the salt) with long polymerization time (24 h) at low temperature (80 ^{o}C) conditions required. This implies that the rate-controlling step in the reaction is the dissolution of the salt. Miyatake and hill found that the cyclization problem in this kind of reaction system can be ameliorated by using a high-speed homogenizer. The high-intensity mixing increased the surface area of the salt, hence aiding its dissolution[9]. Very high molecular weight polyformals with low molecular weight distributions were obtained in a few minutes. In contrast with the typical reactions to synthesize linear poly(aryl ethers), the formation of this specific ladder polymer is more complicated. As can be seen in Scheme **2** both monomers have four reactive groups.

Experimental

Characterization

^{1}H NMR spectrum (400 MHz) of monomers and polymers were recorded on a Bruker DPX 400 spectrometer using $CDCl_3$ as the solvent and tetramethylsilane as the internal standard. FT-IR spectra were recorded on a JASCO FT/IR-6300. Elemental analyses were carried out using Elementar Vario Micro Cube. Mass analyses were done on a Thermo DFS Mass spectrometer. The molecular weight and its distribution were measured by Knauer Gel Permeation Chromatograph fitted with a refractive index detector (flow rate 1 mL/min) according to polystyrene standards using $CHCl_3$ as the eluent. Thermogravimetric analysis (TGA) was performed with a Shimadzu TGA-50 instrument at a heating rate of 10 ^{o}C/min under nitrogen atmosphere and DSC analysis was done on Shimadzu DSC-60 instrument at a heating rate of 10 ^{o}C/min under nitrogen. Melting points were measured with a Griffin melting point apparatus and further confirmed by DSC analysis. Wide-angle X-ray diffraction (WAXD) of films was measured by a Siemens D5000 diffractometer. Microscopic techniques employed are Scanning Electron Microscopy (SEM: JEOL Model 6300) and High Resolution Transmission Electron Microscopy (HRTEM: JEOL Model JEM- 3010). Nitrogen adsorption measurements (77 K) and volumetric hydrogen adsorptions analysis (77 K and 87 K at 1.13 bar) were performed on a Micromeritics ASAP 2020 Sorptometer equipped with an out gassing platform, an online data acquisition and handling system.

Materials

The anhydrous solvents DMF and DMAc were purchased from Aldrich co, and the potassium carbonate obtained from Merck was finely grounded and dried at 200 ^{o}C. 2,3,5,6-tetrachloroterephthalonitrile obtained from aldrich was used directly. TTSBI obtained from alfa was purified from methanol. Starting from tetrachlorophthalic acid, tetrachlorophthalic anhydride was prepared in our laboratory.

Synthesis of chloro-monomers

4,5,6,7-Tetrachloro-2-phenyl-isoindole-1,3-dione. M-Cl**1**

Tetrachlorophthalic anhydride (8.3g, 38.4 mmol) was added to a stirred solution of aniline (2.90g, 32.16 mmol) in glacial acetic acid and refluxed for 3 h. The white solid obtained was further refluxed in acetic anhydride for 12 h. After cooling to room temperature, the precipitated product was filtered off and washed with petroleum ether to give a light yellow solid. Yield: 84 %; Mp 203°C. ^{1}H NMR ($CDCl_3$, δ ppm): 7.15-7.45 (m, 4H, Ar). FTIR (KBr pellet, cm^{-1}): 3088, 1773 (asymmetry C=O), 1746 (symmetry C=O), 1466 (C=C), 1377 (C-N), 788 (C-Cl). Anal. Calcd for $C_{14}H_5NO_2Cl_4$ (361.08): C, 46.94; H, 1.38; N, 3.87. Found: C, 46.55; H, 1.27; N,3.73. MS (EI): m/z (%) 361(100%).

The following monomers were prepared from tetrachlorophthalic anhydride and corresponding amines using similar procedures adopted for M-Cl1

4,5,6,7-Tetrachloro-2-hexyl-isoindole-1,3-dione. M-Cl**2**

Yield: 88 %; Mp 108°C. ^{1}H NMR ($CDCl_3$, δ ppm): 3.55 (t, 2H, CH_2), 1.52-1.69 (m, 2H, CH_2), 1.27-1.33 (m, 6H, CH_2), 0.8 (t, 3H, CH_3). FTIR (KBr pellet, cm^{-1}): 3070, 1770 (asymmetry C=O), 1725 (symmetry C=O), 1445 (C=C), 1358 (C-N), 755 (C-Cl). Anal. Calcd for $C_{14}H_{13}NO_2Cl_4$ (369.26): C, 45.45; H, 3.79; N, 4.62. Found: C, 45.20; H, 4.31; N, 3.79. MS (EI): m/z (%) 369 (100%).

4,5,6,7-Tetrachloro-2-(4-methoxy-phenyl)-isoindole-1,3-dione. M-Cl**3**

Yield: 85 %; Mp 250°C. ^{1}H NMR ($CDCl_3$, δ ppm): 7.18-7.14 (dd, 2H, Ar), 7.18-7.10 (dd, 2H, Ar), 3.81 (s, 3H, CH_3). FTIR (KBr pellet, cm^{-1}): 3070, 2930, 1775 (asymmetry C=O), 1730 (symmetry C=O), 1468 (C=C), 1322 (C-N), 772 (C-Cl). Anal. Calcd for $C_{15}H_7NO_3Cl_4$ (391.03): C, 46.40; H, 1.79; N, 3.51. Found: C, 46.30; H, 1.67; N,3.43. MS (EI): m/z (%) 391 (100%).

4,5,6,7-Tetrachloro-2-trimethoxybenzene-isoindole-1,3-dione. M-Cl**4**

Yield: 87 %; Mp 217°C. ^{1}H NMR ($CDCl_3$, δ ppm): 6.58 (s, 2H, Ar), 3.88 (s, 3H, CH_3), 3.77 (s, 6H, CH_3).FTIR (KBr pellet, cm^{-1}): 3076, 2955, 1766 (asymmetry C=O), 1728 (symmetry C=O), 1462 (C=C), 1350 (C-N), 960 (C-F). Anal. Calcd for $C_{17}H_{11}NO_5Cl_4$ (451.10): C, 52.98; H, 2.89; N, 3.64. Found: C, 52.68; H, 2.78; N, 3.55. MS (EI): m/z (%) 451 (100%).

4,5,6,7-Tetrachloro-2-4-tert -butylbenzene -isoindole-1,3-dione. M-Cl**5**

Yield: 84 %; Mp 221°C. ^{1}H NMR ($CDCl_3$, δ ppm): 7.44-7.41 (dd, 2H, Ar), 7.20-7.18 (dd, 2H, Ar), 1.33 (s, 9H, CH_3). FTIR (KBr pellet, cm^{-1}): 3092, 2945, 1768 (asymmetry C=O), 1735 (symmetry C=O), 1458 (C=C), 1350 (C-N), 871(C-Cl). Anal. Calcd for $C_{18}H_{13}NO_2Cl_4$ (417.1): C, 51.52; H, 3.11; N, 3.33. Found: C, 50.70; H, 3.49; N, 3.30. MS (EI): m/z (%) 417 (45%).

4,5,6,7-Tetrachloro-2-(2,6-diisopropyl-phenyl)-isoindole-1,3-dione. M-Cl**6**

Yield: 92 %; Mp 171°C. ^{1}H NMR ($CDCl_3$, δ ppm): 7.44 (t, H, Ar), 7.33-7.29 (d, 2H, Ar), 2.53 (sept, 2H, CH), 1.17-1.16 (d, 12H, CH_3). FTIR (KBr pellet, cm^{-1}): 3090, 2940, 1770 (asymmetry C=O), 1733 (symmetry C=O), 1450 (C=C), 1350 (C-N) and 770 (C-Cl). Anal. Calcd for $C_{20}H_{17}NO_2Cl_4$ (445.10): C, 63.30; H, 4.48; N, 3.69. Found: C, 63.22; H, 4.36; N, 3.45. MS (EI): m/z (%) 445 (50%).

4,5,6,7-Tetrachloro-1-adamantylamine. M-Cl**7**

Yield: 73%; Mp> 300 ^{o}C. ^{1}H NMR ($CDCl_3$, δ ppm): 2.33 (s, 6H, CH_2), 2.05 (s, 3H, CH), 1.76-1.71 (d, 3H, CH_2), 1.69-1.60 (d, 3H, CH_2). FTIR (KBr pellet, cm^{-1}): 3123, 2921, 1769 (asymmetry C=O), and 1732 (symmetry C=O), 743 (C-Cl). Anal. Calcd for $C_{18}H_{15}NO_2Cl_4$ (419.10): C, 61.17; H, 4.24; N, 3.96. Found C, 60.86; H, 4.40; N, 4.08. MS (EI): m/z (%) 353 (100%).

Synthesis of PIM-Cl(1-7)

PIM-R1

A mixture of monomer M-Cl**1** (0.50g, 1.69 mmol) and spirobiscatechol (0.57g, 1.69 mmol) in dry DMF (70ml) and K_2CO_3 (0.50g, 3.51 mmol) was stirred at 80 ^{o}C for 24 h. After

cooling, the reaction mixture was poured into deionised water and the solid product collected by filtration washed with methanol. The insoluble polymer was then purified by refluxing in methanol and acetone. The obtained yellow fluorescent powder was dried in vacuum oven at 100 ^{o}C for 12h. Yield: 75%. Mp> 300 ^{o}C. Mw 37,403. Mn 35,152. ^{1}H NMR ($CDCl_3$, 298 K δ ppm): 7.48-7.18 (s, br, 3H, Ar), 6.67-6.31 (d, br, 4H, Ar), 2.20 (d, br, 4H, CH_2), 1.28 (s, br, 12H, CH_3). FTIR (KBr pellet, cm^{-1}): 3079, 1770 and 1722 (imide). Anal. Calcd for $C_{35}H_{25}NO_6$ (555.45): C, 75.61; H, 4.50; N, 2.52. Found: C, 75.39; H, 4.63; N, 2.35.

The following polymers were prepared from corresponding chloro-monomers using similar procedure adopted for PIM-Cl1

PIM-Cl2

Yield: 82%. Mp> 300 ^{o}C. Mw 22,624. Mn 10,741. ^{1}H NMR ($CDCl_3$, 298 K, δ ppm): 6.88 (s, br, Ar), 6.48 (s, br, Ar), 3.43 (m, br, 2H, CH_2), 2.08 (d, br, 2H, CH_2), 1.48-1.34 (d, br, 12H, CH_3). FTIR (KBr pellet, cm^{-1}): 3077, 2960, 1777 and 1719 (imide).Anal. Calcd for $C_{35}H_{33}NO_6$ (563.01): C, 74.60; H, 5.86; N, 2.04. Found: C, 74.28; H, 5.77; N, 2.01.

PIM-Cl3

Yield: 84%. Mp> 300 ^{o}C. Mw 37,843. Mn 12,276. ^{1}H NMR ($CDCl_3$, 298 K, δ ppm): 6.88-6.79 (d br, Ar), 6.48 (s br, Ar), 3.77 (t br, OCH_3), 2.26-2.19 (d, br, CH_2), 2.17 (d, 2H, CH_2), 1.31 (s, 12H, CH_3). FTIR (KBr pellet, cm^{-1}): 3090, 1768 and 1717 (imide). Anal. Calcd for $C_{36}NO_7H_{27}$ (585.07): C, 73.84; H, 4.61; N, 2.39. Found: C, 73.48; H, 4.52; N, 2.26.

PIM-Cl4

Yield: 84%. Mp> 300 ^{o}C. Mw 64,278. Mn 54,348. ^{1}H NMR ($CDCl_3$, 298 K, δ ppm): 6.88 (s, 2H, Ar), 6.88-6.48 (m br, , Ar), 3.88-3.77 (m br, OCH_3), 2.22-2.09 (d, CH_2), 1.66 (s, 2H, CH_2), 1.50 (s, 12H, CH_3). FTIR (KBr pellet, cm^{-1}): 1770 and 1742 (imide). Anal. Calcd for $C_{38}H_{31}NO_9$ (645.03): C, 70.69; H, 4.80; N, 2.17. Found: C, 70.57; H, 4.75; N, 2.13.). Anal. Calcd for $C_{38}H_{31}NO_9$ (645.03): C, 70.69; H, 4.80; N, 2.17. Found: C, 70.37; H, 4.71; N, 2.13.

PIM-Cl5

Yield: 86%; Mp> 300 ^{o}C. Mw 66,200. Mn 32,000. ^{1}H NMR ($CDCl_3$, 298 K, δ ppm): 7.44-7.31 (d br, Ar), 6.77-6.40 (d br, Ar), 2.20-2.07 (d br, 4H, CH_2), 1.21-1.14 (d, 21H, CH_3). 3077, 2944, 1771 and 1723 (imide). Anal. Calcd for $C_{39}H_{33}NO_6$ (611.24): C, 76.59; H, 5.40; N, 2.29. Found: C, 76.28; H, 5.32; N, 2.21.

PIM-Cl6

Yiled: 87%. Mp> 300 ^{o}C. Mw 62,594. Mn 57,748. ^{1}H NMR ($CDCl_3$, 298 K, δ ppm): 7.36 (d, 2H, Ar), 6.76 (t br, 2H, Ar), 6.43 (s br, Ar) 2.60 (s br, 2H, CH) 2.24-2.01 (d br, 4H, CH_2) 1.22-1.07 (d, 24H, CH_3). FTIR (KBr pellet, cm^{-1}): 3088, 2945, 1781 and 1727 (imide). Anal. Calcd for $C_{41}H_{37}NO_6$ (641.05): C, 76.90; H, 5.75; N, 2.21. Found: C, 76.79; H, 5.68; N, 2.17

PIM-Cl7

Yield: 80%. Mp> 300 ^{o}C. Mw 22,916. Mn 14,803. ^{1}H NMR ($CDCl_3$, 298 K, δ ppm): 6.74-6.62 (d br, 2H, Ar), 6.36 (s br, 2H, Ar), 2.41-2.29 (t br, CH), 2.11-2.06 (d br, 4H CH_2), 1.69-1.60 (d br, 12H, CH_2), 1.29 (s br, 12H, CH_3). FTIR (KBr pellet, cm^{-1}): 3098, 2960, 1781 and 1709 (imide). Anal. Calcd for $C_{39}H_{35}NO_6$ (613.08): C, 76.30; H, 5.70; N, 2.28. Found: C, 76.08; H, 5.61; N, 2.19.

Results and Discussion

The possibility of the preparation of ladder polymer by the reaction of different tetrachlorophthalimide with 5,5',6,6'-tetrahydroxy-3,3,3',3'-tetramethylspirobisindane (TTSBI) using 4 h and 120 ^{o}C condition[1] consider to result low molecular masses polymer and cyclic by-product. This behavior can be attributed to the presence of cyclic oligomers as a result of the side reactions. It has been reported that in classic polycondensation reactions of bisphenols and bichloro aromatics for the production of poly(aryl ethers) that a large amount of macrocyclic oligomers were formed. [17-18] After many trial, it found that lowering temperature and increasing polymerization time with dilution conditions results high efficient polymerization. The reaction product was characterized by mass, ^{1}H NMR, FTIR spectroscopy and elemental analysis confirming that all the four Cl atoms were replaced by the two benzodioxane units. The highly efficient reaction (yield > 85%) promotes the preparation of microporous organic polymers. The polymers (PIM-Cl[**1-7**]) were synthesized by the dibenzodioxane formation reaction between the TTSBI and various chlorine-containing monomers (MCl[**1-7**]) in dry DMF as illustrated in scheme 1. The polymers were isolated by precipitation in acidified water and the resulting powder samples were purified by refluxing in deionised water, methanol and ethanol respectively followed by reprecipitation in *n*-hexane to give yellow fluorescent powder attributed to the efficiency of the polycondensation reaction. The average molecular masses of prepared polymers were estimated by gel permeation chromatography (GPC) relative to polystyrene standard in $CHCl_3$ (Fig.1). The data obtained from GPC is listed in Table 1. PIM-Cl3, PIM-Cl4 and PIM-Cl6 with relatively high average molecular weight were obtained. The high molecular weight can be attributed to the good solubility of randomly forming polymers in the reaction mixture. On the other hand, GPC curves (See supporting Information) show shoulder peaks in the low molecular weight region while PIM-Cl5 with reasonable molecular weight was obtained in a quantitative yield without any shoulder peak.

Scheme 1

Synthesis of microporous polymers PIM-Cl(1-7)s. Reagents and conditions: Dry DMF, Anhydrous K_2CO_3, 80 ^{o}C, 24 h.

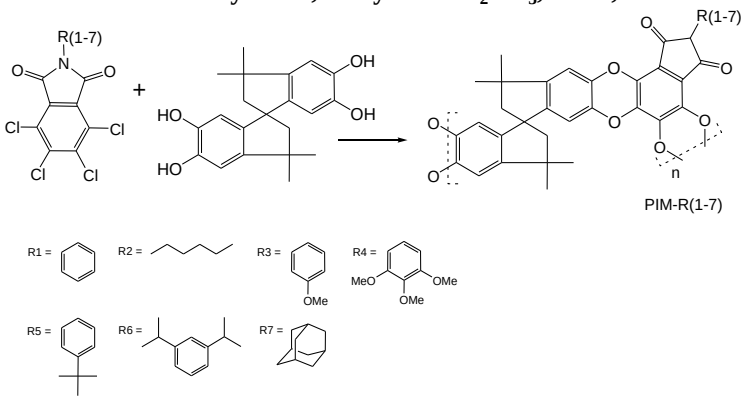

Figure 1.Transparent free standing PIM-Cl6 film

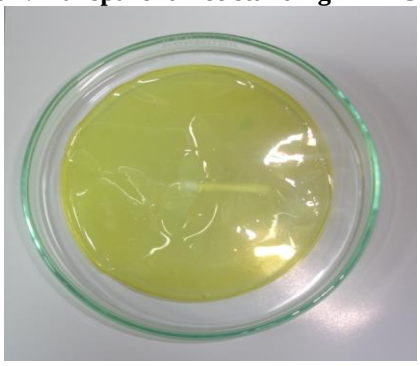

Figure 3. SEM images of PIM-Cl4

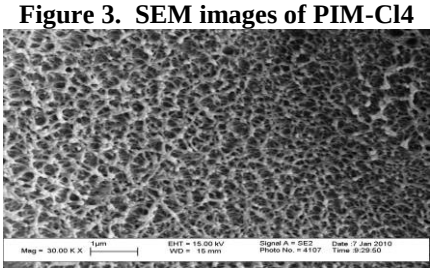

Figure 4. Nitrogen sorption isotherm of PIM-Cl4 at 77K

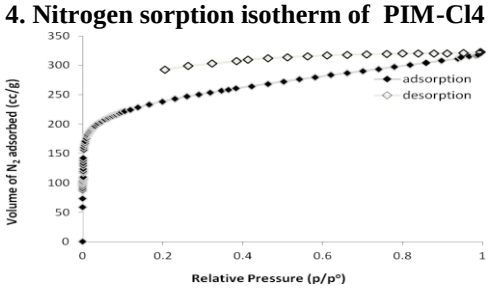

Figure 5. Hydrogen sorption isotherms of PIM-Cl4 at 77K and 87K

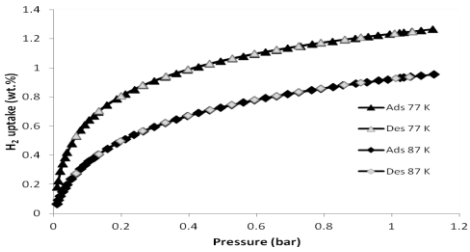

Figure 6. Isosteric heats of adsorption for H_2 on PIM-Cl6

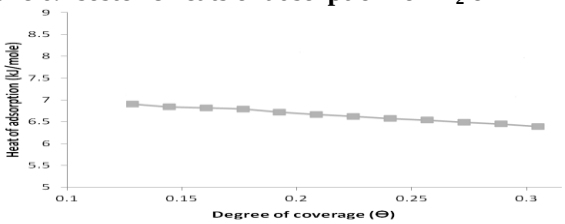

N_2 sorption analysis

The porous nature of PIMs was analyzed by means of nitrogen sorption at 77 K. The most common technique used for screening the porosity involves the fitting of Brunauer-Emmett-Teller (BET) equation to the data obtained from the nitrogen adsorption/desorption isotherms at 77 K. Table 2 lists several relevant parameters obtained from the isotherm analysis including surface areas, micropore area, micropore volume and pore diameter based on Horvath-Kawazoe (HK). The BET surface areas of PIM-Cl(**1**-**7**)s and ranged from 300 to 700 m^2/g, with adequate micropore area (438 to 638 m^2/g). The micropore pore volumes ranging from 0.22 and 0.44 cm^3/g. The difference in specific surface area might be due to the structural geometry of the monomers employed as well as the efficient polycondensation by the incorporation of highly reactive chlorinated monomers into the reaction mixture, resulting in high-molecular-weight copolymers. When comparing the porous properties PIM-Cls which are building up with different monomers and co-monomers, a trend linking porosity and the co-monomer unit can be seen. Typical example of nitrogen adsorption/desorption isotherm is shown in Figure 4. The adsorption isotherms show high uptake at very low relative pressure**,** which is characteristic of a microporous material and isotherms of the prepared polymers exhibit a combination of I and II N_2 sorption isotherm with a continuous increase after the adsorption at low relative pressure and a broad hysteresis upon desorption. Suggesting that, a broad hysteresis down to low pressure is indicative of trapping effect at cryogenic temperature. The extremely low relative pressure portion of the adsorption isotherm is related to the apparent micropore distribution, which in turn is expected to have a profound influence on the transport properties of the polymer. From the *t*-plot analysis it was found that all the prepared polymers showed significant amount of microporosity.

Hydrogen adsorption

The volumetric hydrogen adsorption capacities of all PIMs were measured using a ASAP 2020 instrument with 99.999% pure H_2 over the pressure range 0–1.13 bar. The sorption of hydrogen at cryogenic temperature is also an important tool to identify the microporoisity in polymers. Figure 6 shows the adsorption/desorption isotherms at 77 and 87 K for the PIM-Cl4 with a maximum hydrogen adsorption capacities up to 1.24 and 0.96 wt% respectively at 1.12 bar. The isotherms are fully reversible and exhibit a sharp rise at low pressure region which is consistent with the physisorption of hydrogen on a microporous material. All the prepared PIM-Cls show similar behavior in their isotherm with a significant uptake at two different temperatures (Table 2). From the isotherms it was found that there was no kine tic trapping of hydrogen in small pores upon desorption. The Hydrogen adsorption capacities by various samples with different surface areas usually reveal a linear relationship between BET surface area and H_2 storage capacity at low pressure. For example the H_2 adsorption capacity of PIM-Cl2 (0.79 wt.%) and PIM-Cl4 (1.18 wt.%) at 1 bar and 77 K with their BET surface areas 545 and 719 m^2/g respectively, is consistent with the above hypothesis. Thus from the comparison of various synthesised PIM-Cls and the H_2 adsorption capacities are largely influenced by BET surface area. Several studies showed that a clear relationship exist between total surface area and hydrogen adsorption density of porous material [20-22]. The hydrogen adsorption at 77 K, physisorption mechanism is dominant and the H_2 uptake is controlled by the structural features of the adsorbent material. Moreover small micropores can effectively adsorb hydrogen, probably due to its much smaller kinetic diameter compared to bigger gas molecules such as N_2 [2b,23]. These ultramicropores allow the dihydrogen molecule to interact with multiple portions of the double stranded framework and thereby increasing adsorption potential and a stronger van der Waals interaction with the hydrogen molecules [24,25]. It is therefore clear that the hydrogen storage capacity is generally relative to their respective specific surface areas as well the presence of ultramicroporosity. The langmuir model is frequently used to measure specific surface area of microporous polymers from hydrogen sorption isotherms and the values ranging upto 550 m^2/g as depicted in Table 2. The Langmuir isotherm theory assumes monolayer coverage of adsorbate over a homogenous adsorbent surface of equal energy. The isosteric heat of adsorption,(Q_{st}), for dihydrogen molecules on all samples was calculated from the adsorption isotherms at 77 and 87 K as shown in Figure 5. The calculated Q_{st} values (6.6 to 7.9 kJ/mol) are comparable with other porous organic materials such as COFs , PAFs and HCPs. The highest heat of sorption (7.9 kJ/mol) was observed for PIM-Cl6 indicating a favorable interactions between dihydrogen and polymer surface. As shown in typical example in Figure 6 the values of Q_{st} decreases rapidly as the function of degree of coverage.

Table 1. GPC results and mechanical properties of PIM-Cls

PIMs	M_n	M_w	M_w/M_n
PIM-Cl1	35152	37403	1.27
PIM-Cl2	10741	22624	1.75
PIM-Cl3	37276	12843	2.87
PIM-Cl4	64348	54278	3.09
PIM-Cl5	66000	32200	1.20
PIM-Cl6	62748	57594	2.38
PIM-Cl7	22803	14916	5.50

Table 2. Porous properties of PIM-Cls

PIMs	SA_{BET} (m^2/g)[a]	PV_{micro} (cm^3/g)	HK median pore width (Å)	SA_{LAN} (m^2/g)[b] (77K / 87K)	H_2 (wt.%) at 1.13 bar, (77K/87 K)	Q_{st} (kJ/mole)
PIM-Cl1	650(525)	0.38	7.5	432/323	0.9/0.72	7.24
PIM-Cl2	545 (498)	0.35	6.6	343/275	0.89/0.68	7.35
PIM-Cl3	510 (417)	0.33	8.2	467/353	0.97/0.74	7.14
PIM-Cl4	719 (567)	0.39	7.6	531/436	0.78/0.90	6.85
PIM-Cl5	586 (417)	0.33	8.3	422/315	0.86/0.73	6.66
PIM-Cl6	664 (582)	0.38	6.9	453/326	1.13/0.97	7.24
PIM-Cl7	630 (588)	0.39	6.8	440/346	1.2/0.98	7.37

[a] BET surface area calculated from nitrogen adsorption isotherm. The number in the parathesis is the micropore surface area calculated using the *t*-plot analysis. PV_{micro} is the micropore volume. [b] Surface area calculated from the H_2 adsorption isotherm using Langmuir equation at 77 K and 87 K.

This is attributed to the heterogeneous nature of polymer surface (sorption places are energetically different) which is available for adsorption[2]. In a recent study based on FTIR spectroscopy revealed that the dihydrogen molecules adsorb perpendicular to the surface, the preferential adsorption site is benzene rings.[25,26]

Conclusions

A series of soluble linear polymers exhibiting intrinsic microporosity were synthesized from cheaper chlorinated monomers with TTSBI through nucleophilic substitution reaction condition at 80 ^oC for 24 h. Reaction conditions led to avoid cyclic by-product and high molecular weight polymers which provided surface areas reach to 719 $m^2\ g^{-1}$. The intrinsic microporosity of these polymers is supported by good hydrogen uptake at 77 K and 87 K. Isosteric heat of H_2 adsorption (Q_{st}) measurement revealed that Q_{st} is not highly sensitive to the structural features and exhibit high isoteric heats of adsorption up to 7.9 kJ/mol.

Acknowledgments

I'm grateful for Dr.Saad Makhseed and for financial support from the College of Graduate Studies for my PhD candidacy, and the facilities used from ANALAB, Kuwait University.

References

[1] Saad Makhseed, Fadi Ibrahim, Samuel J. Phthalimide based Polymers of Intrinsic Microporosity. Polymer. 53, **2012**, 2803-3052.

[2] a) Germain, J.; Hradil, J.; Frechet, J. M. J.; Svec, F. Chem Mater 2006, 18, 4430-4435; b) Germain, J.; Svec F.; and Frechet J. M. J. Chem Mater **2008**, 20, 7069–7076.

[3] Ghanem, B. S.; McKeown, N.B.; Harris, K.D.M.; Pan, Z.; Budd, P.M.; Butler, A.; Selbie, J.; Book D.; Walton, A. Chem Commun **2007**, 67-69.

[4] Jiang, Jia-X.; Su, F.; Trewin, A.; Wood, C. D.; Campbell, N. L.; Niu, H.; Dickinson, C.; Ganin, A.Y.; Rosseinsky, M. J., Khimyak Y.Z.; Cooper A.I. Angew Chem Int Ed. **2007**, 44, 8574–8578.

[5] Makhseed S.; Samuel. J. Chem Commun **2008**, 4342- 4344.

[6] Yuan, S.; Dorney, B.; White, D.; Kirklin, S.; Zapol, P.; Yu, L.; Liu, Di-J. Chem Commun 46, **2010**, 4547- 4549.

[7] Wang, Z.; Zhang, B.; Yu, H.; Sun, L.; Jiao, C.; Liu, W. Chem Commun. 46, **2010**, 7730-7732.

[8] McKeown N. B.; Budd P. M. Chem Soc Rev **2006**, 35, 675-683.

[9] Budd, P. M.; Ghanem, B. S.; Makhseed, S.; Mckeown, N. B.; Msayib, K.; Tattershall, C. E.; Wang, D. Chem Commun **2004**, 2, 230-23.

[10]Budd, P.M.; Elabas, E.S.; Ghanem, B.S.; Makhseed, S.; McKeown, N.B.; Msayib, K.J.; Tattershall, C.E.; Wang, D. Advanced Mater **2004**, 16, 456-459.

[11] McKeown, N. B.; Budd, P. M.; Msayib, K.; Ghanem, B. S.; Kingston, H. J.; Tattershall, C. E.; Makhseed, S.; Reynolds, K. J.; Fritsch, D. Chemistry- A European J. **2005**, 11, 2610-2620.

[12] Segmented organosiloxane copolymers. 1. Synthesis of siloxane—urea copolymers İskender YíIgör, Ahmad K. Sha'aban, Warren P. Steckle, Dinesh Tyagi, Garth L. Wilkes, Polymer Volume 25, **1984**, 12, 1800–1806

[13] Thermal polymerization of styrene — the formation of oligomers and intermediates, 1. Discontinuous polymerization up to high conversions K. Kirchner, K. Riederle Die Angewandte Makromolekulare, **1983**, 111, 1–16.

[14] Daniel J. Brunelle . Journal of Polymer Science Part A: Polymer Chemistry, Issue 4, **2008**, 46, 1151–1164.

[15] A. A. Berlin and N. G. Matveyeva Journal of Polymer Science: Macromolecular Reviews Issue 1, **1977**, 12, 1–64.

[16] Yukio ImanishiJournal of Polymer Science: Macromolecular Reviews, Issue 1, **1979**, 14, 1–205

[17] Weber, J.; Du, N.; Guiver, M. D. Macromolecules, **2011**, 44, 1763–1767.

[18] Dawson, R.; Laybourn, A.; Khimyak, Y. Z.; Adams, D.J. and Cooper A. I. Macromolecules **2010**, 43, 8524–8530.

[19] Kricheldorf, H. R.; Schwarz, G. Macromol Rapid Commun. **2003**, 24, 359-381.

[20] Miyatake, K.; Hlil, A. R.; Hay, A. S. Macromolecules **2001**, 34, 4288.

[21] Carta, M.; Raftery, J.; and McKeown, N. B. J. Chem Crystallo **2011**, 41, 98-104.

[20] Dinca, M.; Yu, A. F.; Long, J. R. J. Am Chem Soc. **2006**, 128, 17153–17153.

[21] Foy, A.G.W.; Matzger A.J.; Yaghi, O.M. J. Am Chem Soc. **2006**, 128, 3494–3495.
[22] Mckeown, N.B.; Gahnem, B.; Msayib, K.J.; Budd, P.M.; Tattershall, C.E.; Mahmood, K. Angew Chem Int Ed. **2006**, 45, 1804–1807.
[23] Weber, J.; Antonietti, M.; Thomas, A. Macromolecules, **2008**, 41, 2880–2885.
[24] Shiraishi, M.; Takenobu, T.; Yamada, A.; Ata M.; Kataura, H. Chem Phys Lett. **2002,** 358, 213–218.
[25] G. Yushin, R.K. Dash, J. Jagiello, J.E. Fischer and Y. Gogotsi, Adv Funct Mater. **2006**, 16 2288–2293.
[26] Spoto, G., Vitillo, J.G.; Cocina, D., Damin, A., Bonino, F., and Zecchina, A. Phys. Chem Chem Phys, **2007**, 9, 4992-4999.